

Fatigue Life Evaluation of Joint Designs for Friction Welding of Mild Steel and Austenite Stainless Steel

A. Chennakesava Reddy¹

Professor, Department of Mechanical Engineering, JNTUH College of Engineering
Kukatpally, Hyderabad – 500 085, Telangana, India

Abstract: The purpose of this work was to assess three joints, namely vee-joint, square joint and plain joint, used for joining of dissimilar mild steel and austenite stainless steel materials by continuous drive friction welding. Three joints were evaluated for their strength, hardness, fatigue life, heat affected zone and metal flow across the weld joints. This article dealt with complete failure data (all samples were tested until they failed). The vee-joint found to be the superior alternative for the dissimilar materials in continuous drive friction welding.

Keywords: Joint, mild steel, austenite stainless steel, fatigue, friction welding

1. Introduction

Friction welding is a solid-state welding process that allows material combinations to be joined than with any other welding process. In continuous drive friction welding, one of the workpieces is attached to a motor driven unit while the other is restrained from rotation as showed in figure 1a. The motor driven workpiece is rotated at a predetermined constant speed. The workpieces to be welded are forced together and then a friction force is applied as shown in figure 1b. Heat is generated because of friction between the welding surfaces. This is continued for a predetermined time as showed in figure 1c. The rotating workpiece is halted by the application of a braking force. The friction force is preserved or increased for a predetermined time after the rotation is ceased (figure 1d). Figure 1 also illustrates the variation of welding speed, friction force and forging force with time during various stages of the friction welding process.

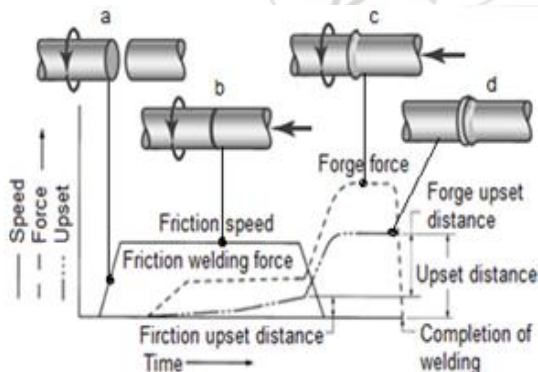


Figure 1: Friction welding

Besides common material combinations such as steel/steel, steel/copper, steel/aluminum or aluminum/magnesium can also be joined without difficulty. With friction welding, joints are possible between not only two solid materials or two hollow parts, but also solid material/hollow part combinations can be reliably welded. However, the shape of a fusion zone in friction welding is dependent the force applied and the rotational speed. If the applied force is too high or the rotational speed is too low, the fusion zone at the centre of the joint will be narrow as showed in figure 2a. On

the other hand, if the applied force is too low or the rotational speed is too high, the fusion zone at the centre of the joint will be wider as showed in figure 2b. In both the cases, the result is poor weld joint strength.

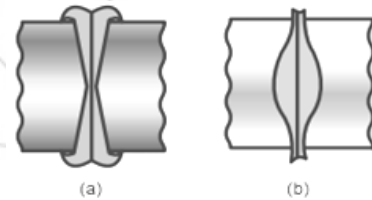


Figure 2: Effect of force and rotational speed in friction welding

In the friction welding process, the developed heat at the interface raises the temperature of workpieces rapidly to values approaching the melting range of the material. Welding occurs under the influence of pressure that is applied when heated zone is in the plastic range, as mentioned [1]. The foremost difference between the welding of similar materials and that of dissimilar materials is that the axial movement is unequal in the latter case whilst the similar materials experience equal movement along the common axis. This problem arises not only from the different coefficients of thermal expansion, but also from the distinct hardness values of the dissimilar materials to be joined. The microstructural evolution of the interface of medium carbon steel/austenitic stainless steel depends on thermo-chemical interactions between the two materials [2]. Joint and edge preparation is very important to produce distortion free welds. The solid-state diffusion is slow in the wider joints [3]. The intermetallic compounds can change the micro hardness near the joint interface of dissimilar metals [4].

Therefore, friction welding of dissimilar metals needs to be eased by ensuring that both the workpieces deform similarly. In this context, this research work aims at modifying the joint design for the joining interface of mild steel/austenite stainless steel, through a systematic study of incorporating uniform material flow at the interface. This research work predicts survivability of distinct joints during the friction welding of mild steel and austenite stainless steel.

2. Experimental Procedure

In order to examine the performance of three proposed joints, mild steel and austenite stainless steel cylindrical bars of 25mm diameter were first cut to the length of about 300mm on an automatic hacksaw machine. The designs of three weld joints namely vee joint, square joint and plain joint are shown in figure 3.

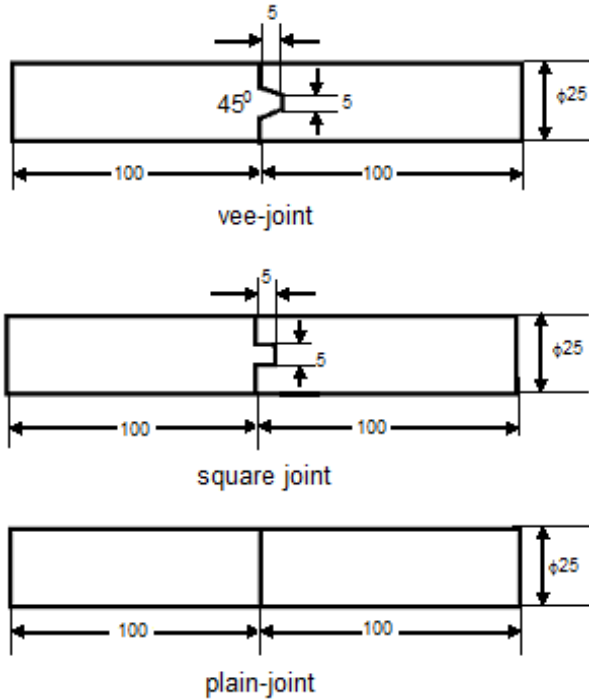


Figure 3: Design of joints

The specimens were machined as per the dimensions of the designed joints (Figure 3) on a lathe machine. After machining operation, these specimens were thoroughly cleaned, washed with distilled water, and finally dried. Friction welding was performed using a pressure servo-controlled brake type machine. The austenite steel workpiece was held on the motor driven unit and the mild steel workpiece was fixed in the static holding device. The machine then was scheduled for its rotational speed as per the intended value and started welding process. Axial movement was then given to mild steel workpiece till both the workpieces come into contact with each other. The welding parameters were rotational speed (4000 rpm), friction pressure (10 ton), friction time (10 sec), upset pressure (20 ton) and upset time (30sec). The welded workpiece was then withdrawn from the machine. A flash, which was built during the welding process, was machined by holding the workpiece in the chuck of the lathe machine. The microstructure of joints was investigated using an optical microscope. The welded specimens were tested for tensile strength on a universal testing machine (UTM). The increase in hardness in the vicinity of the joint was determined in accordance with a Rockwell hardness tester to find the heat affected zone (HAZ). The effect of joint design on HAZ and material flow was also assessed through microstructures.

For the fatigue test, the applied stresses were axial (tension-compression) with low cycle completely reversed constant amplitude where the alternating stress varied from a

maximum tensile stress to a minimum compressive stress of equal magnitude. Ten smooth specimens of each joint were tested under strain controlled conditions in order to evaluate the survival of joints. Geometry and dimensions (ASTM E606) of the fatigue test specimens are shown in figure 4. After machining the specimens to the desired geometry, the specimen surfaces were mechanically polished. The experiments were carried out in a close-loop servo hydraulic test machine with 100 kN load capacity. A sinusoidal waveform was used as a command signal. The fatigue tests were conducted with constant strain amplitudes in atmospheric air conditions. The flashless specimens were cyclic-loaded under strain control with symmetrical push-pull loading, with a nominal strain ratio of 0.1, maximum load of 10KN, a minimum load of -4KN and frequency 10Hz.

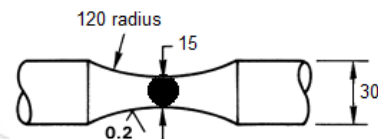


Figure 4: Specimen of fatigue test (all dimensions are in mm).

3. Estimation of Weibull Parameters

Weibull analysis is a method for modeling data sets containing values greater than zero, such as failure data. Weibull analysis can make predictions about the life of a weld joint. The Weibull cumulative distribution function can be transformed so that it is provided in the form of a straight line ($Y=mX+c$). To compute Weibull cumulative distribution the following formulae are used:

$$F(x) = 1 - \exp\left(-\left(\frac{x}{\alpha}\right)^\beta\right) \quad (1)$$

$$1 - F(x) = \exp\left(-\left(\frac{x}{\alpha}\right)^\beta\right)$$

$$\ln\left[\ln\left(\frac{1}{1 - F(x)}\right)\right] = \beta \ln x - \beta \ln \alpha \quad (2)$$

where β is the shape parameter, α is the scale parameter and x is the maximum fatigue cycles.

Comparing Eq.(2) with the simple equation of a line, we see that the left side of Eq.(2) corresponds to Y , $\ln x$ corresponds to X , β corresponds to m , and $-\beta \ln \alpha$ corresponds to c . When the linear regression is performed, the estimate for parameter β comes directly from the slope of the line. The estimate of the parameter α must be calculated as follows:

Comparing Eq.(2) with the simple equation for a line, we see that the left side of Eq.(2) corresponds to Y , $\ln x$ corresponds to X , β corresponds to m , and $-\beta \ln \alpha$ corresponds to c . When the linear regression is performed, the estimate for the parameter β comes directly from the slope of the line. The estimate of the parameter α must be calculated as follows:

$$\alpha = \exp\left(-\left(\frac{b}{\beta}\right)\right) \quad (3)$$

4. Results and Discussion

The microstructure of mild steel (base metal) is shown in figure 5a. The white areas reveal ferrite and dark areas represent pearlite in the mild steel. The microstructure of austenite stainless steel (base metal) is shown in figure 5b. It illustrates the cold worked flow lines parallel to the direction of rolling. The white areas disclose austenite and dark areas stand for ferrite in the austenite stainless steel.

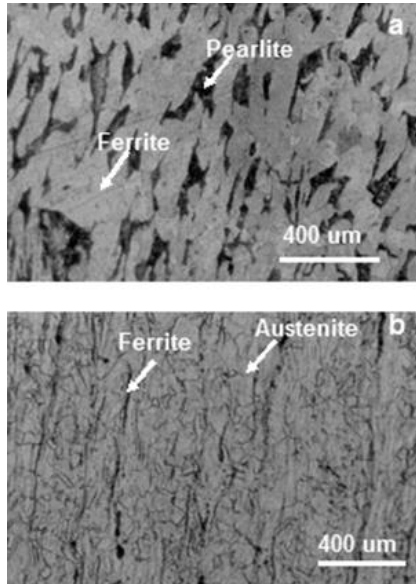


Figure 5: Microstructures of base metals (a) mild steel and (b) austenite stainless steel.

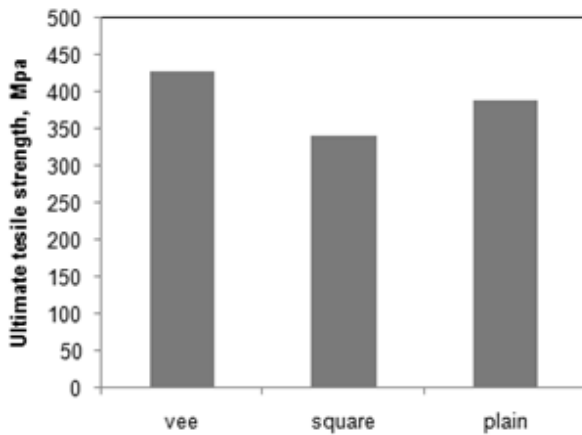


Figure 6: Ultimate tensile strength of joints

4.1 Joint strengths

The surface areas of vee-joint, square joint and plain-joint are A_v , A_s and A_p respectively. Figure 6 shows the ultimate tensile strength of different weld joints. Ultimate tensile strength of vee-joint is greater than of plain-joint and square-joint. The square-joint is under a greater area of contact than vee-joint and plain-joint ($A_s > A_v > A_p$). However, the distribution of upset pressure is not uniform in the square-joint during friction welding due to its profile resulting in poor weld joint. The contact area of vee-joint is greater than of plain-joint ($A_v > A_p$) and smaller than that of square-joint ($A_v < A_s$). In vee-joint, the upset pressure distribution is uniform owing to its profile resulting in good weld joint.

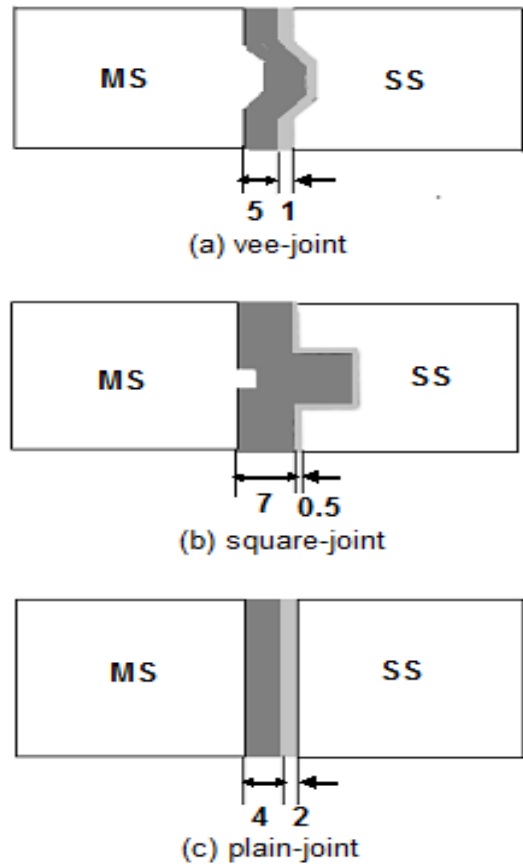


Figure 7: Heat affected zones (HAZ) in different joints

4.2 Heat affected zone (HAZ)

Heat affected zone is that portion of the base metal, where mechanical properties and microstructures are modified by the heat of welding. HAZ is often determined by the response of the weld joint to the hardness or etching effect tests. Friction welding produces very limited and narrow HAZ. Figure 7a shows broad HAZ on the mild steel side. HAZ width from the center line of vee-joint is 5mm for the mild steel and 1mm for the austenite stainless steel. Figure 7b shows that the HAZ width is 7mm on the mild steel side from the center line of square-joint and it is 0.5mm on the austenite stainless steel side. HAZ width is 4mm on the mild steel side from the center line of plane-joint and it is 2mm on the austenite stainless steel side as showed in figure 7c. HAZ width on the mild steel side is double the width on the austenite stainless steel side for the plain-joint. Figure 8 shows the hardness distribution for the weld joints. There increases hardness on the austenite stainless steel slide. The hardness profile across the weld joint shows a sharp peak in the vicinity of weld interface that may affect the properties of the weld joint. The hardness variation for vee-joint in the plasticized zone was lesser than the hardness of base metal because austenite stainless steel was heavily cold worked. The hardness distribution was proved to be higher in the square-joint as compared to the other two joints. Hardness distribution on the austenite stainless steel is greater than of the mild steel side, because the fusion zone is in the mild steel side for all the joints.

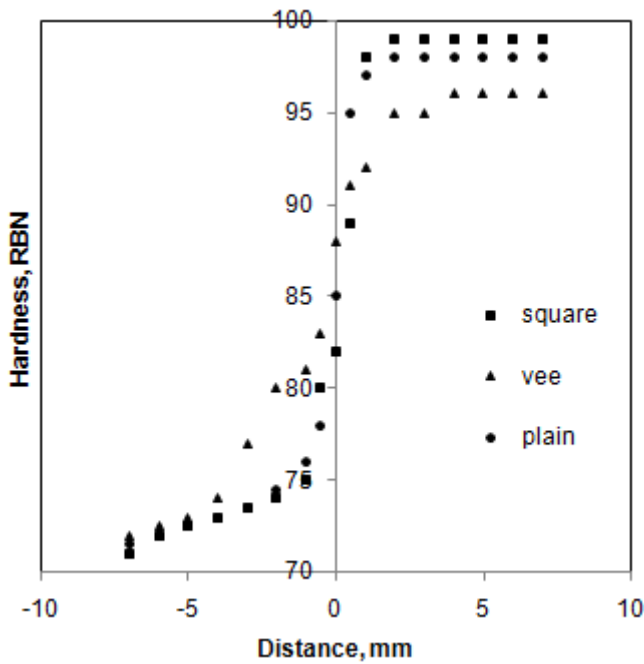


Figure 8: Hardness distributions across the joints

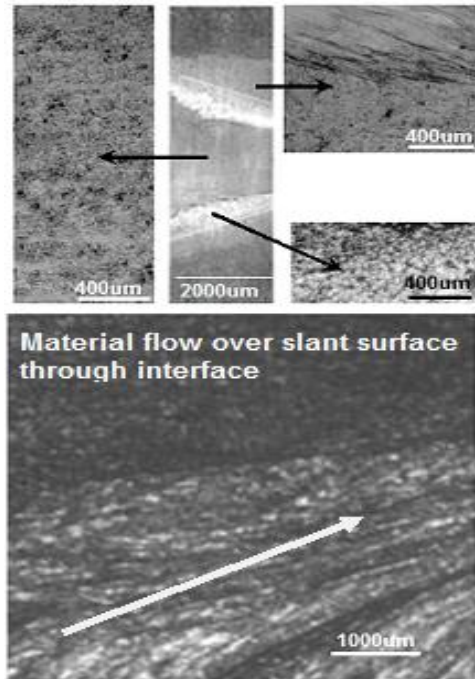


Figure 9: Microstructure and material flow of vee-joint

4.3 Microstructural evaluation of weld joints

Figure 9 reveals the microstructure and material flow of friction welded vee-joint. It shows a nice metal flow and a nice mixture of mild steel and austenite stainless steel materials. Plasticized mild steel slides over the slant surfaces of vee-joint and formed flash on the periphery of specimens as showed in figure 10. The fine grain size structure was obtained at HAZ and weld zones. After cooling and applying the subsequent pressure, the process of recrystallization and growth took place that resulted in a fine grain structure. HAZ was raised to 5m in the mild steel. According to the Hall-Petch equation, material strength depends on the grain size, and the smaller grains produce higher strengths. Figure 11 uncovers the microstructure of friction welded square-joint. It shows no flow of material and there is the absence of

mixing of two materials. The heat affected zone of mild steel reveals fine grained structure. The fusion zone reveals a coarse grain structure. The microstructure on the austenite steel side has not much affected except at the interface because HAZ is extended to 0.5mm only, whereas the same is extended to 7mm on the mild steel side.

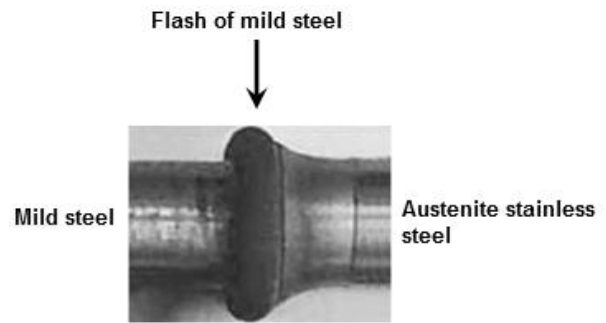


Figure 10: Formation of flash

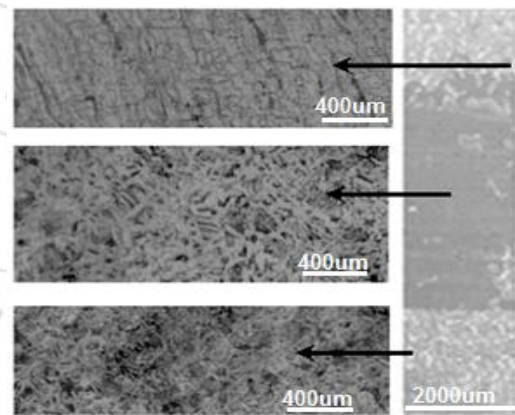


Figure 11: Microstructure and material flow of square-joint

Figure 12 reveals the microstructure of friction welded plain-joint. The partially recrystallised structure is observed on the mild steel side. There is a satisfactory flow pattern of grains on the austenite stainless steel side. In HAZ, the transition is observed from coarse grain pattern of ferrite-pearlite to partially crystallized ferrite-pearlite structure. Microphotograph shows that stainless steel is greatly deformed with grains elongated and refined near the weld interface. The plasticized mild steel slides radially over the plane surface of plain-joint and formed flash on the periphery of specimens.

The microstructure in HAZ and in the interface region of the heat affected zone and fusion zone on the mild steel side is illustrated in figure 13. Refined grain structure in HAZ and coarse grain structure in the fusion zone are noted. Both ferrite and pearlite are observed in the mild steel side. Figure 14 reveals the microstructures in HAZ and in the interface region of the heat affected zone and fusion zone on austenite stainless side. The microstructure in HAZ is not much altered because the extension of HAZ towards the austenite stainless steel side is negligible. However, the interface between the fusion zone and the HAZ has partially crystallized ferrite-pearlite structure.

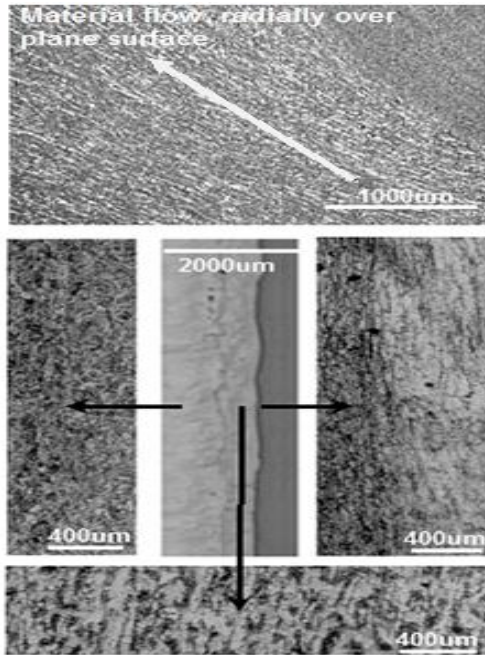


Figure 12: Microstructure and material flow of plain-joint

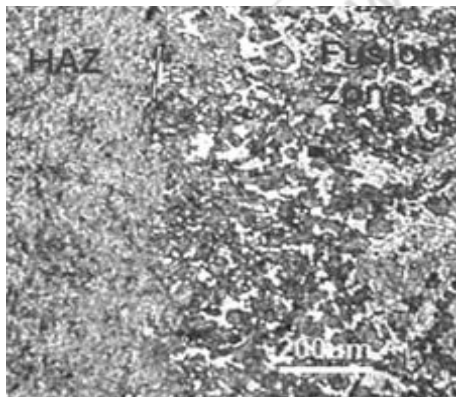


Figure 13: Microstructure on the mild steel side

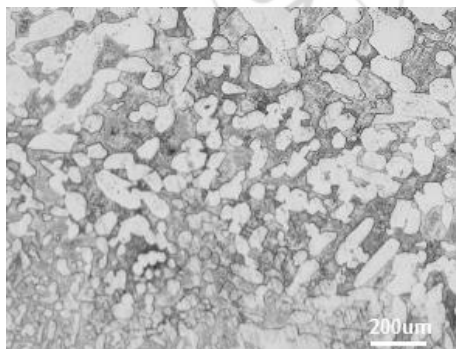


Figure 14: Microstructure on the austenite stainless steel side

4.4 Weibull criteria

The Weibull shape parameter β indicates whether the failure rate is increasing, constant or decreasing. A $\beta < 1.0$ indicates that the product has a decreasing failure rate. This scenario is typical of "infant mortality" and indicates that the joint is failing during its "burn-in" period. A $\beta = 1.0$ indicates a constant failure rate. A $\beta > 1.0$ indicates an increasing failure rate. This is characterized by products that are worn out. Three joint designs: vee-joint, square-joint, and plain-joint

have β values much higher than 1.0 as seen in figure 15. The joints fail due to fatigue, i.e., they wear out. The straight line equation for vee-joint was obtained as:

$$Y = 49.33x - 398.0 \quad (4)$$

The straight line equation for plain-joint was computed as:

$$Y = 46.06x - 350.3 \quad (5)$$

The straight line equation for square-joint was determined as:

$$Y = 59.62x - 452.9 \quad (6)$$

The Weibull characteristic life measures as the scale in the distribution of data. It so happens that α equals the number of cycles of which 63.2 percent of the joint has failed. In other words, for a Weibull distribution $R (= 0.368)$, regardless of the value of β . Survival fatigue cycles for about 37 percent of vee-joints, plane joints, and square joints are respectively 3189, 2497 and 1993.

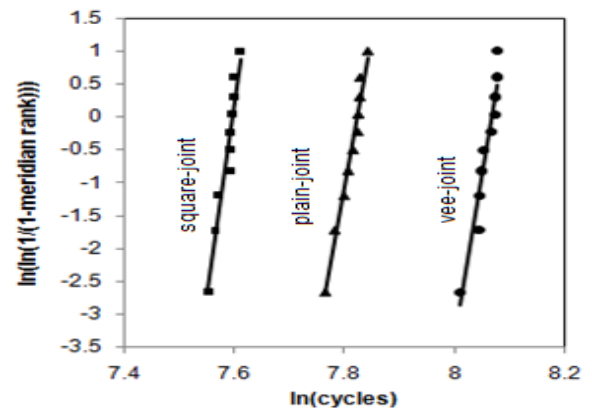


Figure 15: Weibull criterion for joints

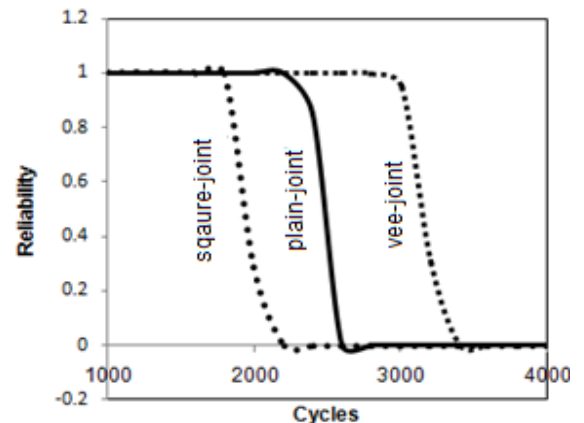


Figure 16: Reliability graphs of joints

Figure 16 permits a comprehensive comparison of survival rates of the three joint designs. At 2500 cycles, about 100 percent of vee-joint welds have survived, whereas only about 35 percent of plain-joint welds have survived and zero percent of square-joint welds have survived. Therefore, for the stated reliability goal of $R(2500) = 1.00$, the vee-joint is clearly superior.

5. Conclusions

This study shows that the vee-joint welds have resulted in higher tensile strength than square and plain joint welds. The metal flow is also good in the vee joint weld. This article proves that alternative weld joints for plain joint are feasible

for the friction welding process. At 2500 cycles, the survivability of vee-joint welds is 100 percent, whereas the survivability of plain-joint welds is 35 percent and the square-joint welds are totally failed.

6. Acknowledgements

The author acknowledges with thanks University Grants Commission (UGC) – New Delhi for sectioning R&D project.

References

- [1] B.S. Yibas, A.Z. Sahin, N. Kahrama, and A.Z. Al-Garni, "Friction welding of St-A1 and Al-Cu materials", *Journal of Materials Processing Technology*, (49), pp.431-443, 1995.
- [2] M. Sahin, and H.E. Akata, "An experimental study on friction welding of medium carbon and austenitic stainless-steel components", *Industrial Lubrication and Tribology*, (56), pp.122-129, 2004.
- [3] A. Chennakesava Reddy, A. Ravaivarma, and V. Thirupathi Reddy, in *Proceedings of National Welding Seminar, IIT-Madras*, pp.51-55, 2002.
- [4] W. Li and F. Wang, "Modeling of continuous drive friction welding of mild steel", *Materials Science and Engineering A*, (528), pp.5921-5926, 2011.

Author Profile



Dr. A. Chennakesava Reddy, B.E., M.E (prod). M.Tech (CAD/CAM), Ph.D (prod), Ph.D (CAD/CAM) is a Professor in Mechanical Engineering, Jawaharlal Nehru Technological University, Hyderabad. The author has published 210 technical papers worldwide. He is the recipient of best paper awards nine times. He is recipient of Best Teacher Award from the Telangana State, India. He has successfully completed several R&D and consultancy projects. He has guided 14 Research Scholars for their Ph.D. He is a Governing Body Member for several Engineering Colleges in Telangana. He is also editorial member of *Journal of Manufacturing Engineering*. He is author of books namely: *FEA, Computer Graphics, CAD/CAM, Fuzzy Logic and Neural Networks, and Instrumentation and Controls*. Number of citations are 516. The total impact factors are 81.734. The author i10-index and h-index are 7 and 19 respectively. His research interests include Fuzzy Logic, Neural Networks, Genetic Algorithms, Finite Element Methods, CAD/CAM, Robotics and Characterization of Composite Materials and Manufacturing Technologies